Collocation Analysis of a Boundary-Layer Model for Crossflow Fractionation Trays

A nonequilibrium model for fractionation trays with lateral dispersion is analyzed by a collocation method. Mobile-interface turbulent boundary-layer theory is used to describe the local heat and mass transfer rates with allowance for vapor superheat, liquid subcooling, and net molar transfer between the phases. Multicomponent transport is incorporated by a linearized matrix method. Numerical integration of the gradients through the tray permits use of local flows and states, as well as local phase equilibrium expressions. A collocation scheme solves the model efficiently; two grid points normally suffice to represent a tray. The model contains just two adjustable coefficients, a_{00} and Pe; the dependence of these on tray geometry and hydrodynamics remains to be investigated.

Thomas C. Young
Warren E. Stewart
Department of Chemical Engineering
University of Wisconsin
Madison, WI 53706

Introduction

Investigations of fractionation tray efficiencies have traditionally been based on simplified physical models, such as the well-mixed tray model, the mixing pool model (Nord, 1946; Gatreaux and O'Connell, 1955), the recirculation model (Oliver and Watson, 1956), or the eddy diffusivity model (AIChE, 1958). Each of these models contains several restrictive assumptions so that analytic solutions can be obtained. Zero net molar interphase transfer is implicit in each of these models; departures may be important for systems with large differences in latent heats. Constant transfer coefficients and linearized phase equilibria are also assumed; departures may be important for nonideal systems. Isothermal models are normally used, prompting speculation about the role of heat transfer on fractionation trays (Danckwerts *et al.*, 1960; Haseldon and Sutherland, 1960; Zhavoronkov *et al.*, 1979; Weiss and Langer, 1979; Smith, 1982).

The well-mixed tray model has been extended to multicomponent systems by Diener and Gerster (1968), Chan and Fair (1984), Krishnamurthy and Taylor (1985), and others, using various interpretations of the film theory. Replacement of the film theory by a linearized boundary-layer approach should give better multicomponent predictions, as illustrated by Young and Stewart (1986). This approach is followed here.

The purpose of this paper is to provide a nonequilibrium model for multicomponent crossflow fractionation trays, using current approaches in transport theory, and to implement this model by an efficient collocation scheme. Such a model can be used to correlate existing data and establish predictive procedures for use in the design and simulation of fractionation systems.

The local heat and mass transfer expressions used in the present model are based on the boundary-layer theory of Stewart *et al.* (1970) and Stewart (1987), developed for turbulent boundary layers at mobile interfaces. This theory predicts the relative transfer resistance of adjacent phases, eliminating the need for separate correlations of gas and liquid transfer coefficients on fractionation trays. The transfer expressions are extended to multicomponent systems by a modification of the linearized matrix method of Stewart and Prober (1964) and Toor (1964). Detailed phase equilibrium expressions are also usable, as the examples demonstrate.

Fractionation Tray Model

The present model for fractionation trays is based on the crossflow pattern indicated in Figure 1. The vapor stream is assumed to flow vertically through the liquid with negligible backmixing. Froth and clear liquid heights, $h_{2\phi}$ and h_L, are assumed uniform across the tray. Material and energy balances on a differential volume of vapor give, in molar units

$$c_G\left(\frac{\partial y_{i\infty}}{\partial t} + v_G^{\star}\frac{\partial y_{i\infty}}{\partial z}\right) = \frac{h_{2\phi}}{(h_{2\phi} - h_L)}\left(N^{\mathrm{I}}_{i0,G} - y_{i\infty}N^{\mathrm{I}}_{T0,G}\right)a(\boldsymbol{r}, t)$$

$$i = 1 \ldots n-1 \quad (1)$$

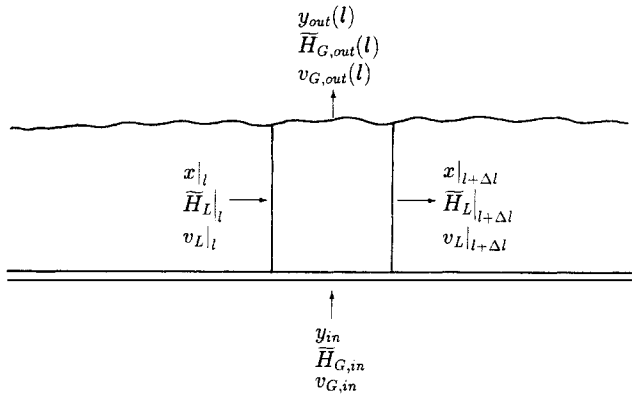

Figure 1. Tray mixing model.

$$c_G\left(\frac{\partial \tilde{H}_{G\infty}}{\partial t} + v_G^\star \frac{\partial \tilde{H}_{G\infty}}{\partial z}\right) = \frac{h_{2\infty}}{(h_{2\phi} - h_L)}\left(e^{\mathrm{I}}_{0,G} - \tilde{H}_{G\infty} N^{\mathrm{I}}_{T0,G}\right) a(\boldsymbol{r}, t) \quad (2)$$

$$\frac{\partial c_G}{\partial t} + \frac{\partial (c_G v_G^\star)}{\partial z} = \frac{h_{2\phi}}{(h_{2\phi} - h_L)} N^{\mathrm{I}}_{T0,G}\, a(\boldsymbol{r}, t) \quad (3)$$

The righthand terms represent the local rates of material and energy transfer into the vapor, per unit vapor volume.

A one-dimensional dispersion model is used for the liquid phase. Splashing is assumed to be the dominant dispersion mechanism, giving the same dispersion coefficient D_E for every species. The liquid is assumed to be well mixed vertically. Material and energy balances on a differential volume of liquid give in molar units

$$c_L\left(\frac{\partial x_{i\infty}}{\partial t} + v_L^\star \frac{\partial x_{i\infty}}{\partial l}\right) = \frac{\partial}{\partial l}\left(c_L D_E \frac{\partial x_{i\infty}}{\partial l}\right) + \frac{1}{h_L}\int_0^{h_{2\phi}} \left(N^{\mathrm{II}}_{i0,L} - x_{i\infty} N^{\mathrm{II}}_{T0,L}\right) a(\boldsymbol{r}, t)\, dz \quad i = 1 \ldots n-1 \quad (4)$$

$$c_L\left(\frac{\partial \tilde{H}_{L\infty}}{\partial t} + v_L^\star \frac{\partial \tilde{H}_{L\infty}}{\partial l}\right) = \frac{\partial}{\partial l}\left(c_L D_E \frac{\partial \tilde{H}_{L\infty}}{\partial l}\right) + \frac{1}{h_L}\int_0^{h_{2\phi}} \left(e^{\mathrm{II}}_{0,L} - \tilde{H}_{L\infty} N^{\mathrm{II}}_{T0,L}\right) a(\boldsymbol{r}, t)\, dz \quad (5)$$

$$\frac{\partial c_L}{\partial t} + \frac{\partial c_L v_L^\star}{\partial l} = \frac{1}{h_L}\int_0^{h_{2\phi}} N^{\mathrm{II}}_{T0,L}\, a(\boldsymbol{r}, t)\, dz \quad (6)$$

The integral terms in Eqs. 4–6 represent the fluxes into the liquid, integrated over the height of the froth.

Although Eqs. 1–6 are reasonable models for macroscopic tray behavior, they are difficult to apply since $v_L^\star$, $v_G^\star$, h_G, $h_{2\phi}$, a, and D_E are not well known. This difficulty is handled here in the customary manner by lumping together unknown quantities and averaging them across the tray. The total concentration in each phase is also assumed to be independent of position, and the multicomponent transport notation described in the appendix is used. Equations 1–6 can then be put into dimensionless forms

$$c_G^*\left(\frac{\partial \xi_{G,\infty}}{\partial t_G^*} + v_G^* \frac{\partial \xi_{G,\infty}}{\partial z^*}\right) = \frac{A_0}{\mathcal{W}_{G,\mathrm{ref}}}\left[\boldsymbol{J}_{G,0} + N_{T0,G}\left(\xi_{G,0} - \xi_{G,\infty}\right)\right] \quad (7)$$

$$\frac{\partial c_G^*}{\partial t_G^*} + c_g^* \frac{\partial v_G^*}{\partial z^*} = \frac{A_0}{\mathcal{W}_{G,\mathrm{ref}}} N_{T0,G} \quad (8)$$

$$c_L^*\left(\frac{\partial \xi_{L,\infty}}{\partial t_L^*} + v_L^* \frac{\partial \xi_{L,\infty}}{\partial l^*} - \frac{1}{Pe}\frac{\partial^2 \xi_{L,\infty}}{\partial l^{*2}}\right) = \frac{A_0}{\mathcal{W}_{L,\mathrm{ref}}}\int_0^1 \left[\boldsymbol{J}_{L,0} + N_{T0,L}\left(\xi_{L,0} - \xi_{L,\infty}\right)\right] dz^* \quad (9)$$

$$\frac{\partial c_L^*}{\partial t_L^*} + c_L^* \frac{\partial v_L^*}{\partial l^*} = \frac{A_0}{\mathcal{W}_{L,\mathrm{ref}}}\int_0^1 N_{T0,L}\, dz^* \quad (10)$$

in which

$$v_G^* = v_G^\star / V_G \qquad c_L^* = c_L / c_{L,\mathrm{ref}}$$
$$l^* = l / l_{\mathrm{tray}} \qquad z^* = z / h_{2\phi}$$
$$c_G^* = c_G / c_{G,\mathrm{ref}} \qquad t_L^* = t V_L / l_{\mathrm{tray}}$$
$$V_L = \frac{\mathcal{W}_{L,\mathrm{ref}} l_{\mathrm{tray}}}{c_{L,ref} h_L A_{\mathrm{tray}}} \qquad Pe = V_L l_{\mathrm{tray}} / D_E$$
$$v_L^* = v_L^\star / V_L \qquad V_G = \frac{\mathcal{W}_{G,\mathrm{ref}}}{c_{G,\mathrm{ref}} A_{\mathrm{tray}}}\left(\frac{h_{2\phi}}{h_{2\phi} - h_L}\right)$$
$$t_G^* = t V_G / h_{2\phi}$$

The coefficient A_0 is a reference area for interphase transfer, to be equated later to A_{tray}.

A matrix expression for the interfacial heat and mass fluxes is developed in the Appendix. Insertion of Eq. A23 into the steady-state versions of Eqs. 7–8 gives

$$v_G^* \frac{\partial \xi_{G,\infty}}{\partial z^*} = \frac{A_0}{\mathcal{W}_{G,\mathrm{ref}}}\left[\boldsymbol{C}_G + \boldsymbol{H}_G\right] \cdot \left[\boldsymbol{k}_G^* + N_{T0,G}\boldsymbol{I}\right]\left[\boldsymbol{C}_G + \boldsymbol{H}_G\right]^{-1}\left(\xi_{G,0} - \xi_{G,\infty}\right) \quad (11)$$

$$\frac{\partial v_G^*}{\partial z^*} = \frac{A_0}{\mathcal{W}_{G,\mathrm{ref}}} N_{T0,G} \quad (12)$$

Under steady-state conditions, Eqs. 9–10 can be rearranged as follows.

$$\frac{1}{Pe}\frac{\partial^2 \xi_{L,\infty}}{\partial l^{*2}} - v_L^* \frac{\partial \xi_{L,\infty}}{\partial l^*} = \frac{\mathcal{W}_{G,\mathrm{ref}}}{\mathcal{W}_{L,\mathrm{ref}}}\left[v_G^*\left(\xi_{G,\infty} - \xi_{L,\infty}\right)\big|_{z^*=1} - v_G^*\left(\xi_{G,\infty} - \xi_{L,\infty}\right)\big|_{z^*=0}\right] \quad (13)$$

$$\frac{\partial v_L^*}{\partial l^*} = -\frac{\mathcal{W}_{G,\mathrm{ref}}}{\mathcal{W}_{L,\mathrm{ref}}}\left(v^*_{G,z^*=1} - v^*_{G,z^*=0}\right) \quad (14)$$

A mass transport equation similar to Eq. 13 was derived by Biddulph (1975), who used a point efficiency expression for the vapor phase.

Equations. 11–14 are subject to the following steady-state boundary conditions.

$$\xi_{G,\infty} = \xi_{G,\text{in}} \quad \text{at} \quad z^* = 0 \tag{15}$$

$$v_G^* = v_{G,0}^* \quad \text{at} \quad z^* = 0 \tag{16}$$

$$\xi_{L,\infty}|_{0+} - \xi_{L,\text{in}} = \frac{1}{Pe}\left.\frac{\partial \xi_{L,\infty}}{\partial l^*}\right|_{0+} \quad \text{at} \quad l^* = 0 \tag{17}$$

$$\frac{\partial \xi_{L,\infty}}{\partial l^*} = 0 \quad \text{at} \quad l^* = 1 \tag{18}$$

$$v_L^* = v_{L,0}^* \quad \text{at} \quad l^* = 0 \tag{19}$$

Equations 17–18 are analogous to the familiar boundary conditions of Danckwerts (1953) for packed bed reactors. Experimental evidence for the jump condition in Eq. 17 has been given by Oliver and Watson (1956) and by Lockett and Ahmed (1983).

Equations 11–19 are more complete than traditional eddy diffusivity models. Heat transfer and net molar fluxes are included directly. Nonideal flow patterns can also be included, if desired, by using position-dependent liquid and vapor velocity functions. State-dependent transfer coefficients can be used. Local vapor-liquid equilibrium expressions can be used, improving the accuracy for nonideal systems.

Interphase Transfer

The transfer models used in previous fractionation studies include the penetration model (Higbie, 1935), the surface-renewal model (Danckwerts, 1951), various eddy diffusivity models (Földes and Evangelidi, 1968; Hughmark, 1971) and annular two-phase flow models (Bakowski, 1952; Young and Weber, 1972; Krishna, 1985). The Higbie and Danckwerts models predict a ½-power dependence of the mass transfer coefficient on diffusivity, in agreement with experimental data for packed and plate columns (Sherwood and Holloway, 1940; Vivian and King, 1964; Mehta and Sharma, 1966; Vidwans and Sharma, 1987; Öztürk *et al.*, 1987).

The penetration and surface-renewal models are logically superseded by the asymptotic analyses of Levich (1962), Ruckenstein (1968), Stewart *et al.* (1970), and Stewart (1987), which use more realistic fluid motions. Stewart *et al.* (1970) provide mobile-interface boundary layer solutions valid for small diffusivities or short contact times, and replace the postulate of surface renewal with a straightforward analysis of the stretching and shrinking of interfacial elements. Stewart (1987) extended the analysis to larger diffusivities and longer exposure times.

The results of Stewart and associates (1970, 1987) are for constant bulk fluid states. Extensions to nonuniform bulk states may be done by averaging the upstream states over all interfaces in a macroscopic volume element. In the first approximation, this gives the same results, except that the main fluid states are replaced by the bulk conditions. Here the modified results thus obtained are applied to fractionation trays.

The extension of the linearized matrix approach of Stewart and Prober (1964) and Toor (1964) to combined multicomponent heat and mass transfer is discussed in the Appendix. Insertion of the results of Stewart *et al.* (1970) into Eq. A24 gives expressions for evaluating the matrix $[\boldsymbol{k}_G^{\bullet} + \boldsymbol{I}N_{T0,G}]$ of Eq. 11. These results are summarized below:

$$\check{k}_{G,i}^{\bullet} = k^{\bullet}(\check{D}_{G,i}, \ldots) = \check{k}_{G,i}\check{\theta}_{G,i} \tag{20}$$

$$\check{k}_{G,i} = c_G \check{D}_{G,i}^{1/2} a_{00} \sqrt{V/L} \tag{21}$$

$$N_{T0,G} = \check{\phi}_{G,1}\check{k}_{G,1} \tag{22}$$

$$\check{\theta}_{G,i} = \frac{\exp\left(-\check{\phi}_{G,i}^2/\pi\right)}{\left[1 + \operatorname{erf}\left(\check{\phi}_{G,i}/\sqrt{\pi}\right)\right]} \tag{23}$$

$$a_{00} = \frac{2}{\sqrt{\pi}}\frac{1}{A_0}\sqrt{L/V} \iint_{\mathcal{R}} \frac{\partial}{\partial t}\sqrt{\int_{t_0(u,w)}^{t} s^2(u, w, t_1)\, dt_1}\; du\, dw \tag{24}$$

Similar equations may be written for the liquid phase by replacing the subscript G with L in Eqs. 20–23. Here a_{00} is a dimensionless function that accounts for the effect of interfacial stretching on the local boundary layer thickness, integrated over the entire liquid-vapor interfacial region $\mathcal{R}(u, w, t)$ of a single tray. The coefficient a_{00} depends only on the interfacial motion, as shown in Eq. 24. However, in practice, a_{00} must be determined and correlated by fitting the theory to experimental data. The function a_{00} is the same for each contiguous phase and is treated here as a pseudosteady function. The reference quantities L and V are chosen here as the outlet weir height, h_W, and inlet superficial vapor velocity, $W_{G,\text{in}}/(c_{G,\text{in}}A_{\text{tray}})$.

This pseudosteady treatment of a_{00} corresponds to the observed behavior of stage efficiencies. The corresponding pseudosteadiness of the integral in Eq. 24 is attributed to the dominant role of the expanding surface elements, whose stretching offsets the increasing ages $[t - t_0(u, w)]$ of their boundary layers as in the examples given by Stewart *et al.* (1970). The local value $t_0(u, w)$ may be regarded as the birth time for the present boundary layer alongside the surface element (u, w). This is either the time of initiation of the phase contacting, or (if the local surface element has contracted and later expanded) $t_0(u, w)$ may be regarded as the time when the element completed its latest contraction (and consequent ejection of its former boundary layers into the adjoining phases).

Surface renewal (Danckwerts, 1951) does not arise in this continuum treatment. However, the boundary-layer ejection and the subsequent flow of bulk fluid toward such interfacial elements as they start to grow, constitute a boundary-layer "rejuvenation" process somewhat like that proposed by Danckwerts (1955) as an alternative to surface renewal.

Equations 21 and 22, and their liquid-phase analogs give the relations

$$\check{\phi}_{G,i} = \left(\frac{\check{D}_{G,1}}{\check{D}_{G,i}}\right)^{1/2} \check{\phi}_{G,1} \tag{25}$$

$$\check{\phi}_{L,i} = -\frac{c_G}{c_L}\left(\frac{\check{D}_{G,1}}{\check{D}_{L,i}}\right)^{1/2} \check{\phi}_{G,1} \tag{26}$$

among the net flux measures, $\check{\phi}_{G,i}$ and $\check{\phi}_{L,i}$. Furthermore, the normal fluxes relative to the interface satisfy the conservation conditions

$$\begin{bmatrix} N_{1,0} \\ \cdot \\ \cdot \\ \cdot \\ N_{n-1,0} \\ e_0 \end{bmatrix}_G = - \begin{bmatrix} N_{1,0} \\ \cdot \\ \cdot \\ \cdot \\ N_{n-1,0} \\ e_0 \end{bmatrix}_L \tag{27}$$

Substitution of Eqs. A19, A23 and 20 into Eq. 27 gives the relation

$$[\boldsymbol{C}_L + \boldsymbol{H}_L]\boldsymbol{P}_L \operatorname{diag}\left\{\frac{k_{L,i}}{k_{G,1}}\check{\theta}_{L,i} - \check{\phi}_{G,1}\right\} \cdot \boldsymbol{P}_L^{-1}[\boldsymbol{C}_L + \boldsymbol{H}_L]^{-1}(\xi_{L,0} - \xi_{L,\infty}) + [\boldsymbol{C}_G + \boldsymbol{H}_G]\boldsymbol{P}_G \operatorname{diag}\left\{\frac{k_{G,i}}{k_{G,1}}\check{\theta}_{G,i} + \check{\theta}_{G,i}\right\} \cdot \boldsymbol{P}_G^{-1}[\boldsymbol{C}_G + \boldsymbol{H}_G]^{-1}(\xi_{G,0} - \xi_{G,\infty}) + \check{\phi}_{G,1}(\xi_{G,\infty} - \xi_{L,\infty}) = 0 \tag{28}$$

after division by $k_{G,1}$. The interfacial equations are completed with generalized equilibrium local expressions.

$$\xi_{G,0} = \boldsymbol{F}(\xi_{L,0}, p) \tag{29}$$

$$\tilde{H}_L = \tilde{H}_{\text{bub}}(\xi_{L,0}, p) \tag{30}$$

Reduction of fractionation data with Eqs. 11–30 requires correlation of just two dimensionless quantities, a_{00} and Pe, as functions of the hydrodynamic variables.

Collocation Procedures

A fast solution method is needed to solve Eqs. 11–30, since column simulation methods will require many solutions. Collocation is chosen here to achieve computational speed, with tailor-made basis functions to allow a coarse spatial grid.

Eqs. 11, 12, 15 and 16 may be abbreviated as

$$\frac{d\boldsymbol{S}_G}{dz^*} = \boldsymbol{f}_G(\boldsymbol{S}_G, \boldsymbol{S}_L) \tag{31}$$

$$\boldsymbol{S}_G(0) = 0 \tag{32}$$

in which $\boldsymbol{S}_G$, $\boldsymbol{S}_L$, and $\boldsymbol{f}_G$ are the following column vectors:

$$\boldsymbol{S}_G = \begin{Bmatrix} \xi_{G,\infty} - \xi_{G,\text{in}} \\ v_G^* - v_{G,0}^* \end{Bmatrix} \qquad \boldsymbol{S}_L = \{\xi_{L,\infty} - \xi_{L,\text{in}}\}$$

$$\boldsymbol{f}_G = \frac{A_0}{\mathcal{W}_{G,\text{ref}}} \begin{Bmatrix} [\boldsymbol{C}_G + \boldsymbol{H}_G][\boldsymbol{k}_G^* + N_{T0,G}\boldsymbol{I}] \\ [\boldsymbol{C}_G + \boldsymbol{H}_G]^{-1}(\xi_{G,0} - \xi_{G,\infty})/v_G^* \\ N_{T0,G} \end{Bmatrix}$$

The liquid equations (Eqs. 13, 14 and 17–19) may be similarly abbreviated as

$$\frac{1}{Pe}\frac{d^2\boldsymbol{S}_L}{dl^{*2}} - v_L^*\frac{d\boldsymbol{S}_L}{dl^*} = \boldsymbol{f}_L(\boldsymbol{S}_L) \tag{33}$$

$$\frac{dv_L^*}{dl^*} = g_L(\boldsymbol{S}_L) \tag{34}$$

$$\boldsymbol{S}_L(0) = \frac{1}{Pe}\frac{d\boldsymbol{S}_L}{dl^*}\bigg|_0 \tag{35}$$

$$\frac{d\boldsymbol{S}_L}{dl^*}\bigg|_1 = 0 \tag{36}$$

$$v_L^*(0) = 1 \tag{37}$$

in which

$$\boldsymbol{f}_L(\boldsymbol{S}_L) = \frac{\mathcal{W}_{G,\text{ref}}}{\mathcal{W}_{L,\text{ref}}} \cdot [(v_{G,\text{in}}^* - v_{G,z^*=1}^*)\xi_{L,\infty} + v_{G,z^*=1}^*\xi_{G,\infty,z^*=1} - v_{G,\text{in}}^*\xi_{G,\text{in}}] \tag{38}$$

$$g_L(\boldsymbol{S}_L) = -\frac{\mathcal{W}_{G,\text{ref}}}{\mathcal{W}_{L,\text{ref}}}(v_{G,z^*=1}^* - v_{G,\text{in}}^*) \tag{39}$$

The collocation procedure is to approximate the state vectors as truncated series,

$$\tilde{\boldsymbol{S}}_G(l^*, z^*) = \sum_{i=1}^{N_{\text{COL},G}} \boldsymbol{a}_i(l^*)\varphi_{G,i}(z^*) \tag{40}$$

$$\tilde{\boldsymbol{S}}_L(l^*) = \sum_{i=1}^{N_{\text{COL},L}} \boldsymbol{b}_i\varphi_{L,i}(l^*) \tag{41}$$

with adjustable coefficients $\boldsymbol{a}_i(l^*)$ and $\boldsymbol{b}_i$, and basis functions $\varphi_{G,i}(z^*)$ and $\varphi_{L,i}(l^*)$. A grid is imposed on the spatial region of interest, as shown in Figure 2, and these expansions are made to satisfy the governing equations of the model at each grid point. Since the liquid is assumed to be well mixed vertically, the liquid equations are solved just once at each value of l^*.

The vapor state solutions are expected to be exponential-like, so a method like that of Guertin *et al.* (1977) is used. In this

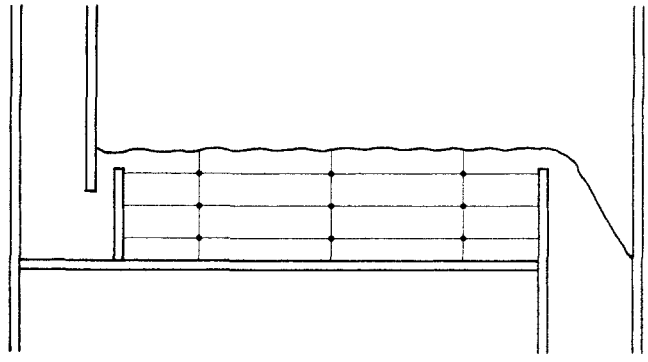

Figure 2. Collocation grid.

method, the righthand side of Eq. 31 is initially approximated as a linear Taylor expansion in S_G. Substitution into Eq. 31 and repeated integration yield a solution that is a linear combination of the following vector basis functions.

$$\varphi_{G,1} = [\exp\{[\Lambda]z^*\} - I]b \tag{42}$$

$$\varphi_{G,i} = z^{*i-1} \exp\{[\Lambda]z^*\}b \quad i = 2, 3, \ldots \tag{43}$$

Here $[\Lambda] = \partial f_G/\partial S_G$ and $b = f_G(S_{G,\text{ref}}, S_L) - [\Lambda]S_{G,\text{ref}}$. The exponential matrix functions in Eqs. 42–43 are evaluated here via the series techniques reviewed by Taylor and Webb (1981). Approximating S_G as a series of these basis functions, $\varphi_{G,i}$, is equivalent to approximating the forcing function in Eq. 13 as

$$f_G(S_G, S_L) \doteq f_G(\tilde{S}_{G,\text{ref}}, \tilde{S}_L) + [\Lambda](\tilde{S}_G - \tilde{S}_{G,\text{ref}}) + \Sigma_i \beta_i(l^*)\, \varphi_{G,i}(z^*) \tag{44}$$

An alternative, also tested here, is to expand $f_G(S_G, S_L)$ in powers of z^*. It turns out, as shown later, that Eq. 44 gives comparable accuracy with fewer terms and hence, with less computing effort.

Liquid-phase basis functions are constructed by solving approximate versions of Eqs. 33 and 34, with polynomial forcing functions, and imposing the boundary conditions. Separate basis functions are required to approximate S_L and v_L^*, since the governing equations are different. The basis functions for S_L are defined by the equations

$$\frac{1}{Pe}\frac{d^2\varphi_{L,i}}{dl^{*2}} - \frac{d\varphi_{L,i}}{dl^*} = l^{*(i-1)} \tag{45}$$

$$\varphi_{L,i}(0) = \frac{1}{Pe}\left.\frac{d\varphi_{L,i}}{dl^*}\right|_0 \tag{46}$$

$$\left.\frac{d\varphi_{L,i}}{dl^*}\right|_1 = 0 \tag{47}$$

giving

$$\varphi_{L,i} = \left(\sum_{j=1}^{i} \frac{(i-1)!}{(j-1)!} Pe^{j-i-1}\right) e^{Pe(l^*-1)} - \left(\sum_{j=0}^{i} \frac{(i-1)!}{j!} Pe^{j-i}\, l^{*j}\right) \tag{48}$$

Similar treatment of Eq. 34 gives the basis functions $\varphi_{FL,i}(l^*) = l^{*i}$ for representing the total liquid flow.

It is convenient to do the collocation in terms of grid-point values, rather than compute the coefficients in the series approximation. The derivatives at the grid points are then expressed as follows:

$$\left.\frac{d\tilde{S}_G}{dz^*}\right|_{z_j^*} = \sum_{k=1}^{N_{\text{COL},G}} A_{G,jk}\, \tilde{S}_G(z_k^*) \tag{49}$$

$$\left.\frac{d\tilde{S}_L}{dl^*}\right|_{l_m^*} = \sum_{p=1}^{N_{\text{COL},L}} A_{L,mp}\, \tilde{S}_L(l_p^*) \tag{50}$$

$$\left.\frac{d^2\tilde{S}_L}{dl^{*2}}\right|_{l_m^*} = \sum_{p=1}^{N_{\text{COL},L}} E_{L,mp}\, \tilde{S}_L(l_p^*) \tag{51}$$

$$\left.\frac{d\tilde{v}_L^*}{dl^*}\right|_{l_m^*} = \sum_{p=1}^{N_{\text{COL},L}} A_{FL,mp}\, \tilde{v}_L^*(l_p^*) \tag{52}$$

The weights, $A_{G,jk}$, $A_{L,mp}$, $A_{FL,mp}$, and $E_{L,mp}$, are computed by requiring that Eqs. 49–52 be satisfied at the grid points for the expansions in Eqs. 40 and 41. Insertion of Eqs. 49–52 into Eqs. 31, 33 and 34 then gives the collocation equations

$$\sum_{k=1}^{N_{\text{COL},G}} A_{G,jk}\tilde{S}_G(z_k^*, l_m^*) = f_G(\tilde{S}_G(z_j^*, l_m^*), \tilde{S}_L(l_m^*)) \tag{53}$$

$$\sum_{p=1}^{N_{\text{COL},L}} \left[\frac{1}{Pe} E_{L,mp} - \tilde{v}_L^*(l_m^*)\, A_{L,mp}\right] \cdot \tilde{S}_L(l_p^*) = f_L[\tilde{S}_L(l_m^*), \ldots] \tag{54}$$

$$\sum_{p=1}^{N_{\text{COL},L}} A_{FL,mp}\, [\tilde{v}_L^*(l_p^*) - 1] = g_L\, [\tilde{S}_L(l_m^*), \ldots] \tag{55}$$

which are solved by Newton's method. The notation . . . denotes vapor phase states shown in Eqs. 38 and 39. Local vapor states at $z^* = 1$ are required to evaluate $f_L[S_L(l_j^*), \ldots]$ and are found by extrapolation of Eq. 40.

Overall material and energy balances are used to calculate the state and flow rate of the mixed vapor rising from the tray.

$$\tilde{v}_G^*\tilde{S}_{Gi}^*|_{\text{out}} - \tilde{v}_G^*\tilde{S}_{Gi}^*|_{\text{in}} = \int_0^1 (\tilde{v}_G^*\tilde{S}_{Gi}^*|_{z^*=1} - \tilde{v}_G^*\tilde{S}_{Gi}^*|_{z^*=0})\, dl^*$$

$$i = 1, \ldots n = \sum_{p=1}^{N_{\text{COL},L}} W_p\, (\tilde{v}_G^*\tilde{S}_{Gi}^*|_{z^*=1,l_p^*} - \tilde{v}_G^*\tilde{S}_{Gi}^*|_{z^*=0,l_p^*}) \tag{56}$$

$$\tilde{v}_G^*|_{\text{out}} - \tilde{v}_G^*|_{\text{in}} = \int_0^1 (\tilde{v}_G^*|_{z^*=1} - \tilde{v}_G^*|_{z^*=0})\, dl^* = \sum_{p=1}^{N_{\text{COL},L}} W_p\, (\tilde{v}_G^*|_{z^*=1,l_p^*} - \tilde{v}_G^*|_{z^*=0,l_p^*}) \tag{57}$$

Two choices are considered here for the collocation points in z^* and l^*: the zeros of a Legendre polynomial on the interval [0, 1] and those of a suitable Radau polynomial on the same interval. The latter chioce allows a collocation point to be placed at an exit surface so that the exit state of the relevant stream is directly included in the grid. These two chioces are natural for polynomial basis functions and are also reasonable for exponentials of moderate steepness. Formulas and tables of Legendre and Radau polynomial zeros are given in Kopal (1961).

Computation Procedure

The collocation equations (Eqs. 53–55) and the interfacial state equations (Eqs. 28–30) are solved simultaneously for the state vector $(\xi_{G,0}, \xi_{L,0}, \dot{\phi}_{G,1}, S_G, S_L, v_L^*)$ at each grid point using Newton's method. Initial estimates for the bulk liquid and vapor states are made by interpolation using the basis functions $\varphi_{G,1}$ and $\varphi_{L,1}$. Initial estimates for the interfacial states are made by assuming that $\xi_{L,0} = \xi_{L,\infty}$ and that the vapor is in equilibrium with the liquid at the interface.

Table 1. Data for First Test Problem

Stream	Jeganathan (1981) run 26, $p = 1.0162$ bar				
	x_{CH_3OH}	x_{H_2O}	$T(K)$	$T_{sat}(K)$	F(mol/s)
Liquid In	0.8425	0.1575	336.65	340.28	7.65
Liquid Out	0.6490	0.3510	345.75	343.67	7.45
Vapor In	0.6490	0.3510	352.05	352.02	7.45
Vapor Out	0.8462	0.1538	344.45	343.82	7.65

In our first example, we consider the experimental data of Jeganathan (1981), measured with the apparatus described by Lockett and Ahmed (1983). They measured the performance of a 0.6M diameter crossflow sieve tray for the distillation of methanol and water. Test 26 of Jeganathan (1981) is summarized in Table 1. This test was chosen because of the large changes in composition and the nonideal vapor-liquid equilibrium behavior to provide a stringent convergence test of the collocation procedure with the various basis functions.

Thermodynamic properties were calculated by the methods recommended by Prausnitz *et al.* (1980). The virial equation of state was used for the vapor phase, and the UNIQUAC activity model was used for the liquid phase. The polynomial equations recommended by Prausnitz *et al.* (1980) for ideal gas heat capacities were used. Pure component vapor pressures were calculated using the Antoine equation, with the parameters recommended by Reid *et al.* (1977). Methanol-water UNIQUAC binary interaction parameters were estimated from the data of Newsham (1981). The thermodynamic consistency of these data was discussed by Jeganathan (1981), who found them to be more reliable than previous data. Liquid molar volumes were estimated using the modified Rackett equation. Vapor transport properties were calculated from kinetic theory, with collision integrals modified for polar contributions. Soret and Dufour coefficients were assumed to be negligible. Liquid thermal conductivity and binary diffusivities were calculated from temperature corrections to available data, using the methods recommended by Reid *et al.* (1977).

The well-mixed liquid model was used to test the convergence of the vapor collocation methods. The parameter value $a_{00} = 173.3$ was chosen to give outlet conditions close to the experimental results. The outlet liquid state and tray efficiency predicted by using polynomial collocation for the vapor are listed in Table 2 and those found by exponential collocation are shown in Table 3. Both techniques converge quickly, attaining the roundoff limit with six or fewer collocation points. Collocation at the Legendre zeros is more accurate than use of the Radau zeros, as expected. The fastest convergence is obtained using the exponential basis functions at the Legendre zeros; one collocation point gives good results.

Table 3. Convergence of Exponential Vapor Collocation Method

No. of Points	Predicted Liquid Outlet State					Predicted
	x_{CH_3OH}	x_{H_2O}	$T(K)$	$T_{sat}(K)$	L(mol/s)	$E_{MV}(\%)$
	Legendre Collocation Points					
1	0.649134	0.350866	343.752	343.664	7.5004	96.821
2	0.659011	0.350989	343.755	343.666	7.5003	96.907
3	0.649005	0.350995	343.756	343.666	7.5003	96.911
	Radau Collocation Points					
1	0.649145	0.350845	343.753	343.664	7.5005	96.815
2	0.648978	0.351022	343.756	343.667	7.5003	96.930
3	0.649004	0.350996	343.756	343.666	7.5003	96.911

The liquid collocation techniques were also tested against the data of Table 1. The experimental value of 9.845 given by Jeganathan (1981) was used for the Peclet number. The parameter value $a_{00} = 89.0$ was chosen for this model to give outlet conditions close to the experimental results. Polynomial collocation at four Legendre points was used for the vapor phase to ensure good vapor-phase convergence for this problem. The outlet liquid state and tray efficiency predicted by the liquid polynomial collocation methods are listed in Table 4. Reasonable convergence is shown, each method reaching the roundoff limit with eight or fewer collocation points. Collocation at the Legendre zeros gives faster convergence of the predicted tray efficiency. Reasonable accuracy is obtained using only two Legendre points.

In our second example, we consider the experimental data of Dribika (1986), as summarized by Biddulph *et al.* (1986). They

Table 2. Convergence of Polynomial Vapor Collocation Method

No. of Points	Predicted Liquid Outlet State					Predicted
	x_{CH_3OH}	x_{H_2O}	$T(K)$	$T_{sat}(K)$	L(mol/s)	$E_{MV}(\%)$
			Legendre Collocation Points			
1	0.609998	0.390002	344.509	344.399	7.4736	126.888
2	0.654956	0.345044	343.624	343.556	7.5039	92.788
3	0.648588	0.351412	343.764	343.674	7.5001	97.205
4	0.649023	0.350977	343.755	343.666	7.5003	96.898
5	0.649005	0.350995	343.756	343.666	7.5003	96.911
6	0.649005	0.350995	343.756	343.666	7.5003	96.911
			Radau Collocation Points			
1	0.678465	0.321535	343.200	343.126	7.5247	77.544
2	0.640382	0.359618	343.920	343.826	7.4943	103.073
3	0.650065	0.349935	343.736	343.647	7.5009	96.169
4	0.648941	0.351059	343.757	343.667	7.5003	96.956
5	0.649007	0.350993	343.756	343.666	7.5003	96.909
6	0.649005	0.350995	343.756	343.666	7.5003	96.911

Table 4. Convergence of Liquid Collocation Method

No. of Points	Predicted Liquid Outlet State					Predicted
	x_{CH_3OH}	x_{H_2O}	$T(K)$	$T_{sat}(K)$	L(mol/s)	E_{MV}(%)
	Legendre Collocation Points					
1	0.648191	0.351809	345.157	343.681	7.5105	97.622
2	0.649159	0.350841	342.974	343.663	7.4963	96.751
3	0.649108	0.350892	344.149	343.664	7.5044	96.891
4	0.649011	0.350989	343.703	343.666	7.5012	96.919
5	0.649030	0.350970	343.866	343.666	7.5024	96.920
6	0.659022	0.350978	343.806	343.666	7.5020	96.920
7	0.649026	0.350974	343.827	343.666	7.5021	96.920
8	0.659025	0.350975	343.820	343.666	7.5021	96.920
	Radau Collocation Points					
1	0.669323	0.330677	343.445	343.293	7.5191	83.222
2	0.648013	0.351987	343.847	343.685	7.5013	97.630
3	0.648856	0.351144	343.810	343.669	7.5018	97.037
4	0.649005	0.350995	343.838	343.666	7.5022	96.935
5	0.649021	0.350979	343.812	343.666	7.5020	96.922
6	0.649025	0.350975	343.827	343.666	7.5021	96.920
7	0.649024	0.350976	343.818	343.666	7.5021	96.920
8	0.649025	0.350975	343.823	343.666	7.5021	96.920

measured the performance of a 0.083M by 0.991M rectangular sieve tray for the distillation of methanol, ethanol and *n*-propanol. Test K3R of Dribika (1986) was chosen for comparison of the collocation techniques. Stream states for this problem are listed in Table 5. This test was chosen because of the large observed Peclet number and multicomponent effects that cause an apparently negative Murphree tray efficiency for ethanol. These features should also provide a difficult test of the convergence of the collocation techniques. Dribika (1986) provides only liquid state data. The listed vapor stream states were inferred from a total recycle mass balance. The inlet vapor stream was assumed to be at its dew point, since temperatures were not provided.

Table 5. Data for Second Test Problem

Stream	Dribika (1986) run K3R, p = 1.0132 bar					
	x_{MeOH}	x_{EtOH}	x_{n-PrOH}	$T(K)$	$T_{sat}(K)$	F(mol/s)
Liquid in	0.3365	0.4741	0.1894	348.05	348.24	1.078
Liquid out	0.1635	0.4799	0.3566	353.35	353.27	1.058
Vapor in	0.1635	0.4799	0.3566	358.15	358.09	1.058
Vapor out	0.3365	0.4741	0.1894	353.25	352.81	1.078

Thermodynamic and physical properties for this example were calculated using the same techniques discussed earlier. Binary UNIQUAC interaction parameters were found using the data of Delzenne (1958), Amer *et al.* (1956), and Dribika (1986).

The liquid collocation techniques were used to model test K3R of Dribika (1986). The experimental value of 39 given by Biddulph *et al.* (1986) was used for the Peclet number. The parameter value a_{00} = 45.6 was chosen to give outlet a_{00} mole fractions close to the experimental values Exponential collocation at one Legendre point was used for the vapor phase; this was found to provide reasonable vapor-phase convergence for this problem. The predicted outlet liquid state and tray efficiencies are listed in Table 6. The liquid collocation techniques converge somewhat less quickly than in the first example, probably because of the larger Peclet number and higher tray efficiency. Still, reasonable convergence is obtained using two Legendre collocation points. The agreement between predicted and observed mole fractions is good, showing that the model is able to handle complicated multicomponent effects.

Conclusions

A generalized model and numerical procedure have been presented here for simulation of multicomponent fractionation trays. The examples show the ability of the method to handle multicomponent mass and heat transfer on a crossflow tray.

Table 6. Convergence of Liquid Collocation Method

No. of Pts.	Predicted Liquid Outlet State						Predicted Efficiency		
	x_{MeOH}	x_{EtOH}	x_{n-PrOH}	T (K)	T_{sat} (K)	L (mol/s)	$E_{MV,1}$ (%)	$E_{MV,2}$ (%)	$E_{MV,3}$ (%)
				Legendre Collocation Points					
1	0.152368	0.481963	0.365669	353.223	353.603	1.0547	171.574	−14.963	110.437
2	0.163762	0.475097	0.361141	353.402	353.333	1.0564	138.392	−2.806	104.814
3	0.163563	0.475284	0.361153	353.646	353.337	1.0569	138.964	−3.250	104.891
4	0.163511	0.475275	0.361213	353.420	353.338	1.0564	139.029	−3.230	104.911
5	0.163507	0.475289	0.361204	353.545	353.338	1.0567	139.073	−3.261	104.926
6	0.163487	0.475289	0.361224	353.486	353.339	1.0566	139.106	−3.261	104.936
7	0.163486	0.475292	0.361222	353.512	353.339	1.0566	139.117	−3.268	104.940
8	0.163482	0.475292	0.361226	353.502	353.339	1.0566	139.121	−3.267	104.941
				Radau Collocation Points					
1	0.197175	0.467255	0.335569	352.595	352.385	1.0602	81.164	60.061	79.892
2	0.161796	0.476277	0.361927	353.545	353.379	1.0565	143.449	−5.460	105.798
3	0.163243	0.475358	0.361399	353.505	353.346	1.0566	139.709	−3.414	105.135
4	0.163375	0.475325	0.361299	353.513	353.342	1.0566	139.387	−3.342	105.026
5	0.163436	0.475306	0.361257	353.500	353.340	1.0566	139.234	−3.299	104.977
6	0.163466	0.475298	0.361236	353.508	353.340	1.0566	139.164	−3.281	104.955
7	0.163477	0.475294	0.361229	353.502	353.339	1.0566	139.136	−3.272	104.946
8	0.163481	0.475293	0.361226	353.506	353.339	1.0566	139.126	−3.269	104.943

Nonzero net molar transfer, variable transport coefficients, large changes in composition and temperature, and nonideal vapor-liquid equilibrium behavior are all accommodated by the method. Inlet streams that depart from saturation can also be handled.

The new collocation method allows efficient solution of the distributed model; two collocation points per tray are normally sufficient to give reasonable accuracy. Incorporation of this method into column models should allow realistic, yet efficient, simulation of fractionation column behavior.

The present model should be useful for correlation of fractionation tray data. The model contains just two adjustable coefficients, a_{00} and Pe, to be represented as functions of tray geometry and hydrodynamic variables. This representation remains to be investigated in future research.

Acknowledgment

This research was supported by Grant No. DE-FG02-84ER13291 from the U.S. Department of Energy, Office of Basic Energy Sciences, and by an AMOCO Foundation fellowship awarded to Thomas C. Young.

Appendix: Matrix Methods for Combined Heat and Mass Transfer

Matrix methods are often employed to solve multicomponent heat and mass transfer problems. DeLancey (1967) modified the diagonalization procedure of Stewart and Prober (1964) and Toor (1964) to include heat transfer. Tambour and Gal-Or (1976) used matrix methods to analyze boundary-layer transport of energy and species when kinetic energy terms were important. Krishna and Standart (1979) gave a detailed solution of the one-dimensional film model. In this appendix, the combined energy and species continuity equations are written in forms that ensure diagonability of the extended diffusion coefficient matrix, allowing the equations to be decoupled after a suitable linearization.

The diagonalization methods of Stewart and Prober (1964) and Toor (1964) may easily be extended to combined heat and mass transfer. For isobaric systems without viscous dissipation or homogeneous reactions, the energy and species continuity equations are, in molar units

$$c\tilde{C}_p\left(\frac{\partial T}{dt} + \boldsymbol{v}^\star \bullet \nabla T\right) = -\nabla \bullet \boldsymbol{q}^\star + \sum_{i=1}^{n-1} H_{xi} \nabla \bullet \boldsymbol{J}_i^\star \quad \text{(A1)}$$

$$c\left(\frac{\partial x_i}{dt} + \boldsymbol{v}^\star \bullet \nabla x_i\right) = -\nabla \bullet \boldsymbol{J}_i^\star \qquad i = 1 \ldots n-1 \quad \text{(A2)}$$

The flux equations for combined heat and mass transfer are

$$\boldsymbol{J}_i^\star = -c\sum_{j=1}^{n-1} D_{ij} \nabla x_j - cD_{iT} \nabla T \qquad i = 1 \ldots n-1 \quad \text{(A3)}$$

$$\boldsymbol{q}^\star = -c\tilde{C}_p \sum_{j=1}^{n-1} D_{Tj} \nabla x_j - c\tilde{C}_p \alpha \nabla T + \sum_{i=1}^{n-1} H_{xi} \boldsymbol{J}_i^\star \quad \text{(A4)}$$

The coefficients D_{ij} are the multicomponent diffusivities, whereas D_{Tj} and D_{iT} are Dufour and Soret coefficients, respectively. The elements of the partial enthalpy vector, $\boldsymbol{H}_x$, are

$$H_{xi} = \left(\frac{\partial \tilde{H}}{\partial x_i}\right)_{T,P,x_{j\neq i,n}} = \overline{H}_i - \overline{H}_n \quad \text{(A5)}$$

Substitution of Eqs. A3–A4 into Eqs. A1 and A2 gives

$$c\left(\frac{\partial \xi'}{dt} + \boldsymbol{v}^\star \bullet \nabla \xi'\right) = \nabla \bullet c\boldsymbol{D} \nabla \xi' + \frac{1}{\tilde{C}_p}\{\nabla[\boldsymbol{C} + \boldsymbol{H}]\} \bullet c\boldsymbol{D} \nabla \xi' \quad \text{(A6)}$$

Here ξ' is the state vector $[x_1, \cdots x_{n-1}, T]\dagger$ and

$$\boldsymbol{C} = \begin{bmatrix} \boldsymbol{I}_{n-1} & \boldsymbol{0} \\ \boldsymbol{0} & \tilde{C}_p \end{bmatrix} \quad \text{(A7)}$$

$$\boldsymbol{H} = \begin{bmatrix} \boldsymbol{0} & 0 \\ \boldsymbol{H}_x^\dagger & 0 \end{bmatrix} \quad \text{(A8)}$$

$\boldsymbol{D}$ is an expanded diffusion coefficient matrix.

$$\boldsymbol{D} = \begin{bmatrix} D_{1,1} & \cdots & D_{1,n-1} & D_{1,T} \\ \cdot & & \cdot & \cdot \\ \cdot & & \cdot & \cdot \\ \cdot & & \cdot & \cdot \\ D_{n-1,1} & \cdots & D_{n-1,n-1} & D_{n-1,T} \\ D_{T,1} & \cdots & D_{T,n-1} & \alpha \end{bmatrix} \quad \text{(A9)}$$

The multicomponent mass and energy fluxes relative to $\boldsymbol{v}^\star$ are given by

$$\boldsymbol{J} = -c[\boldsymbol{C} + \boldsymbol{H}]\, \boldsymbol{D} \nabla \xi' \quad \text{(A10)}$$

Here $\boldsymbol{J}$ is the flux vector $[\boldsymbol{J}_1^\star, \ldots \boldsymbol{J}_{n-1}^\star, \boldsymbol{q}^\star]\dagger$.

The combined equations may be more concisely represented by replacing the temperature T with the molar enthalpy $\tilde{H}$ in the state vector. The energy and species continuity equations then become

$$c\left(\frac{\partial \xi}{dt} + \boldsymbol{v}^\star \bullet \nabla \xi\right) = \nabla \bullet c\boldsymbol{D}_H \nabla \xi \quad \text{(A11)}$$

and the flux expression is

$$\boldsymbol{J} = -c\boldsymbol{D}_H \nabla \xi \quad \text{(A12)}$$

Here ξ is the state vector $[x_1, \ldots x_{n-1}, \tilde{H}]\dagger$ and the diffusion coefficient matrix is given by

$$\boldsymbol{D}_H = [\boldsymbol{C} + \boldsymbol{H}]\, \boldsymbol{D}\, [\boldsymbol{C} + \boldsymbol{H}]^{-1} \quad \text{(A13)}$$

The diffusion coefficient matrix, $\boldsymbol{D}$, is diagonable,

$$\boldsymbol{P}^{-1}\boldsymbol{D}\boldsymbol{P} = \text{diag}\,\{\check{D}_1, \ldots \check{D}_n\} \quad \text{(A14)}$$

with real eigenvalues, $\check{D}_1, \ldots \check{D}_n$, which are nonnegative for stable thermodynamic states. Since Eq. A13 is a similarity transformation, $\boldsymbol{D}_H$ has the same eigenvalues as $\boldsymbol{D}$. If the physical properties c, $\boldsymbol{C}$, $\boldsymbol{D}$ and $\boldsymbol{H}$ are assumed constant, Eq. A6 or A11 may be decoupled, giving

$$\left(\frac{\partial \check{\xi}_i}{dt} + \boldsymbol{v}^\star \bullet \nabla \check{\xi}_i\right) = \check{D}_i \nabla^2 \check{\xi}_i \quad i = 1 \ldots n \tag{A15}$$

$$\check{\boldsymbol{J}}_i = -c\check{D}_i \nabla \check{\xi}_i \quad i = 1 \ldots n \tag{A16}$$

Here

$$\check{\boldsymbol{J}} = \boldsymbol{P}^{-1}[\boldsymbol{C} + \boldsymbol{H}]^{-1} \boldsymbol{J} \tag{A17}$$

and

$$d\check{\xi} = \boldsymbol{P}^{-1} d\check{\xi}' = \boldsymbol{P}^{-1}[\boldsymbol{C} + \boldsymbol{H}]^{-1} d\xi \tag{A18}$$

Boundary conditions are often imposed as conditions on the fluxes relative to some coordinate system, stationary or moving. The expression for fluxes relative to stationary coordinates in the enthalpy-mole fraction notation is

$$\begin{bmatrix} \boldsymbol{N} \\ \boldsymbol{e} \end{bmatrix} = \boldsymbol{J} + \left(\sum_{i=1}^{n} \boldsymbol{N}_i\right) \xi \tag{A19}$$

A reference state must be introduced for thermodynamic consistency in the temperature-mole fraction notation:

$$\begin{bmatrix} \boldsymbol{N} \\ \boldsymbol{e} \end{bmatrix} = \boldsymbol{J} + \left(\sum_{i=1}^{n} \boldsymbol{N}_i\right) \{[\boldsymbol{C} + \boldsymbol{H}](\xi' - \xi'_{\text{ref}}) + \xi_{\text{ref}}\} \tag{A20}$$

Equation A20 includes the assumption of constant $\boldsymbol{C}$ and $\boldsymbol{H}$. Variable properties can be handled by replacing this expression with an integral state difference.

If the transformed boundary conditions for a problem are manageable, multicomponent heat and mass transfer solutions may be constructed by superposition of known results for heat transfer in pure fluids or for mass transfer in isothermal binary mixtures.

Binary mass transfer expressions are often given in terms of material transfer coefficients, $k_x^\bullet$, defined by

$$J^\star_{A0} = k_x^\bullet (\mathcal{D}_{AB}, \ldots)(x_{A0} - x_{A\infty}) \tag{A21}$$

Corresponding multicomponent expressions may be obtained by rewriting Eq. A21 in the notation of Eqs. A15–A18 and then combining in matrix form.

$$\check{\boldsymbol{J}}_0 = \text{diag}\{k_x^\bullet (\check{D}_i, \ldots)\}(\check{\xi}_0 - \check{\xi}_\infty) \tag{A22}$$

The original variables may be recovered by inserting Eq. A18 and the inverse of Eq. A17 into Eq. A22. This gives

$$\begin{aligned} \boldsymbol{J}_0 &= [\boldsymbol{C} + \boldsymbol{H}]\, \boldsymbol{k}^\bullet (\xi'_0 - \xi'_\infty) \\ &= [\boldsymbol{C} + \boldsymbol{H}]\, \boldsymbol{k}^\bullet [\boldsymbol{C} + \boldsymbol{H}]^{-1} (\xi_0 - \xi_\infty) \end{aligned} \tag{A23}$$

for the fluxes of species and enery, with

$$\boldsymbol{k}^\bullet = \boldsymbol{P}\, \text{diag}\{k_x^\bullet (\check{D}_i, \ldots)\}\, \boldsymbol{P}^{-1} \tag{A24}$$

Equation A24 corresponds to a superposition of n related binary mass transfer functions, all evaluated for the same molar average velocity field, $v^\star$. This formulation is convenient for fractionation problems, where the net molar fluxes are expected to be small. Similar equations may be written in mass or volumetric units.

Notation

a = local tray interfacial area per unit liquid volume, L^{-1}
a_{00} = hydrodynamic parameter, Eq. 26
A_{jk} = collocation weight
A_0 = reference area of a tray, L^2
A_{Tray} = tray area, L^2
c = concentration, mol/L^3
$\tilde{C}_p$ = heat capacity, $L^2 \cdot Mt^{-2} \cdot T^{-1} \cdot mol^{-1}$
$\boldsymbol{C}$ = matrix in Eq. A7
$\mathcal{D}_{AB}$ = binary diffusivity, L^2/t
$\check{D}_i$ = ith eigenvalue of $\boldsymbol{D}$
D_E = dispersion coefficient, L^2/t
$\boldsymbol{D}$ = matrix in Eq. A9
e_0 = normal energy flux relative to inferface, M/t^3
e = energy flux relative to stationary coordinates, M/t^3
E_{jk} = collocation weight
E_{MV} = Murphree vapor efficiency
$h_{2\phi}$ = froth height, L
h_L = clear liquid height, L
h_W = outlet weir height, L
$\tilde{H}$ = molar enthalpy, $M \cdot L^2 \cdot t^{-2} \cdot mol^{-1}$
$\overline{H}_i$ = partial molar enthalpy, $M \cdot L^2 \cdot t^{-2} \cdot mol^{-1}$
$\boldsymbol{H}$ = partial enthalpy matrix, Eq. A8
$\boldsymbol{I}$ = identity matrix
$\boldsymbol{J}$ = $[J_1^\star, \ldots J_{n-1}^\star, q^\star]\dagger$, column vector of fluxes relative to $\boldsymbol{v}^\star$
$J_i^\star$ = species molar flux relative to $\boldsymbol{v}^\star$, mol/L^2
k_x = molar transfer coefficient for binary mixture, $mol/L^2 \cdot t$
$\boldsymbol{k}$ = transfer coefficient matrix
l = downstream coordinate for liquid, L
l_{tray} = tray length
L = reference length
N_0 = normal molar flux relative to interface, $mol/L^2 \cdot t$
$\boldsymbol{N}$ = molar flux relative to stationary coordinates, $mol/L^2 \cdot t$
p = pressure, M/Lt^2
Pe = tray dispersion Peclet number
$\boldsymbol{P}$ = matrix of column eigenvectors of $\boldsymbol{D}$
$q^\star$ = conductive energy flux relative to $\boldsymbol{v}^\star$, M/t^3
r = position vector, L
s = scale factor in element of interfacial area, $s\, du\, dw$
$\boldsymbol{S}$ = extended state vector, Eqs. 31 and 33
t = time
T = temperature
u, w = imbedded interfacial coordinates
$\boldsymbol{v}^\star$ = molar average velocity, L/t
V = reference velocity, L/t
W_k = collocation weight
$\mathcal{W}$ = molar flowrate, mol/t
x = liquid mole fraction
y = vapor mole fraction
z = vertical coordinate, L

Greek letters

α = thermal diffusivity, L^2/t
$\check{\phi}_i$ = dimensionless net molar flux, $\Sigma_{j=1}^{n} N_{j0}/\check{k}_i$
φ = collocation trial function
$\check{\theta}$ = net-flux correction for element i of the diagonalized transfer coefficient matrix
ξ' = state vector, $[x_1, \ldots x_{n-1}, T]\dagger$
ξ = state vector, $[x_1, \ldots x_{n-1}, \tilde{H}]\dagger$

Subscripts

A, B = chemical species in a binary system
G = gas phase
i, j, k = chemical species or transformed quantities in a multicomponent system or summation indices
L = liquid phase
0 = interfacial state
∞ = bulk state
bub = bubble point

Superscripts

* = dimensionless quantity
˜ = transformed quantity, Eqs. A14, A18 and A22
† = transposed array
• = corrected for net material flux
• = relative to molar average velocity

Literature Cited

Amer, H. H., R. R. Paxton, and M. Van Winkle, "Methanol-Ethanol-Acetone Vapor-Liquid Equilibrium," *I.E.C.*, **48,** 142 (1956).

American Institute of Chemical Engineers, *Bubble Tray Design Manual,* AIChE, New York (1958).

Bakowski, S., "A New Method for Predicting the Plate Efficiency of Bubble-Cap Columns," *Chem. Eng. Sci.*, **1,** 266 (1952).

Biddulph, M. W., "Multicomponent Distillation Simulation—Distillation of Air," *AIChE J.*, **21,** 327 (1975).

Biddulph, M. W., M. M. Dribika, and M. A. Kalbassi, "Multicomponent Efficiencies in Two Types of Distillation Columns," *AIChE J.*, **34,** 618 (1988).

Chan, H., and J. R. Fair, "Prediction of Point Efficiencies on Sieve Trays," *I.E.C. Proc. Des. Dev.*, **23,** 814, 820 (1984).

Danckwerts, P. V., "Significance of Liquid-Film Coefficients in Gas Absorption," *I.E.C.*, **43,** 1460 (1951).

———, "Continuous Flow Systems. Distribution of Residence Times," *Chem. Eng. Sci.*, **2,** (1953).

———, "Gas Absorption Accompanied by Chemical Reaction," *AIChE J.*, **1,** 456 (1955).

Danckwerts, P. V., H. Sawistowski, and W. Smith. "The Effects of Heat Transfer and Interfacial Tension in Distillation," *International Symposium on Distillation, I.Ch.E. Symp. Ser.*, P. A. Rottenburg, ed., **6,** 7 (1960).

DeLancey, G. B., "An Analysis of Non-Isothermal Multicomponent Diffusion in the Liquid Phase," PhD Thesis, Univ. Pittsburgh, Pittsburgh, (1967).

Delzenne, A. O., "Vapor-Liquid Equilibrium Data for Ternary System Methanol-Ethanol-Water," *I.E.C. Chem. Eng. Data Ser.*, **3,** 224 (1958).

Diener, D. A., and J. A. Gerster, "Point Efficiencies in Distillation of Acetone-Methanol-Water," *I.E.C. Proc. Des. Dev.*, **7,** 339 (1968).

Dribika, M. M., "Multicomponent Distillation Efficiencies," PhD Diss., Univ. Nottingham, UK (1986).

Földes, P., and I. Evangelidi, "Efficiency of Turbogrid-Tray Distillation Columns," *Brit. Chem. Eng.*, **13,** 1291 (1968).

Gatreaux, M. F., and H. E. O'Connell, "Effect of Length of Liquid Path on Plate Efficiency," *Chem. Eng. Prog.*, **51,** 232 (1955).

Guertin, E. W., J. P. Sorensen, and W. E. Stewart, "Exponential Collocation of Stiff Reactor Models," *Comp. and Chem. Eng.*, **1,** 197 (1977).

Haseldon, G. G., and I. P. Sutherland, "A Study of Plate Efficiencies in the Separation of Ammonia-Water Systems," *International Symposium on Distillation, I.Ch.E. Symp. Ser.*, P. A. Rottenburg, ed., **6,** 27 (1960).

Higbie, R., "The Rate of Absorption of a Pure Gas into a Still Liquid during Short Periods of Exposure," *Trans. AIChE*, **31,** 365 (1935).

Hughmark, G. A., "Models for Vapor-Phase and Liquid-Phase Mass Transfer on Distillation Trays," *AIChE J.*, **17,** 1295 (1971).

Jeganathan, A. G. R., "Mass Transfer Studies on a Pilot Plant Distillation Column," PhD Diss. UMIST, Manchester, UK (1981).

Kopal, Z., *Numerical Analysis,* Wiley, New York (1961).

Krishna, R., "Model for Prediction of Point Efficiencies for Multicomponent Distillation," *Chem. Eng. R&D,* **63,** 312 (1985).

Krishna, R., and G. L. Standart, "Mass and Energy Transfer in Multicomponent Systems," *Chem. Eng. Commun.*, **3,** 201 (1979).

Krishnamurthy, R., and R. Taylor, "A Nonequilibrium Model of Multicomponent Separations Processes," *AIChE J.*, **31,** 449, 456, 1973 (1985).

Levich, V. G., *Physicochemical Hydrodynamics,* Prentice-Hall, Englewood Cliffs, NJ (1962).

Lockett, M. J., and I. S. Ahmed, "Tray and Point Efficiencies from a 0.6 Metre Diameter Distillation Column," *Chem. Eng. Res. Des.*, **61,** 110 (1983).

Mehta, V. D., and M. M. Sharma, "Effect of Diffusivity on Gas-Side Mass Transfer Coefficient," *Chem. Eng. Sci.*, **21,** 361 (1966).

Newsham, D. M. T., "Thermodynamic Properties of Water, Methanol, Propan-2-ol and Their Mixtures," Internal Report, UMIST, Manchester, UK (1981).

Nord, M., "Plate Efficiencies of Benzene-Toluene-Xylene Systems in Distillation," *Trans. Inst. Chem. Eng.*, **42,** 863 (1946).

Oliver, E. D., and C. C. Watson, "Correlation of Bubble Cap Fractionating Column Plate Efficiencies," *AIChE J.*, **2,** 18 (1956).

Öztürk, S. S., A. Schumps, and W. D. Deckwer, "Organic Liquids in a Bubble Column: Holdups and Mass Transfer Coefficients," *AIChE J.*, **33,** 1473 (1987).

Prausnitz, J., T. Anderson, E. Grens, C. Eckert, R. Hsieh, and J. O'Connell, *Computer Calculations for Multicomponent Vapor-Liquid and Liquid-Liquid Equilibria,* Prentice-Hall, Englewood Cliffs, NJ (1980).

Reid, R. C., J. M. Prausnitz, and T. K. Sherwood, *The Properties of Gases and Liquids, McGraw-Hill, New York (1977).*

Ruckenstein, E., "A Generalized Penetration Theory for Unsteady Convective Mass Transfer," *Chem. Eng. Sci.*, **23,** 363 (1968).

Sherwood, T. K., and F. A. L. Holloway, "Performance of Packed Towers—Liquid Film Data for Several Packings," *AIChE Trans.*, **10,** 39 (1940).

Smith, W., "Thermal Distillation in Differential Contact Columns," *I.Ch.E. Symp. Ser.*, **73,** L1 (1982).

Stewart, W. E., "Forced Convection in Three-Dimensional Flows: IV. Asymptotic Forms for Laminar and Turbulent Transfer Rates," *AIChE J.*, **33,** 2008; **34,** 1030 (1987).

Stewart, W. E., J. B. Angelo, and E. N. Lightfoot, "Forced Convection in Three-Dimensional Flows: II. Asymptotic Solutions for Mobile Interfaces," *AIChE J.*, **16,** 771 (1970).

Stewart, W. E., and R. Prober, "Matrix Calculations of Multicomponent Mass Transfer in Isothermal Systems," *I.E.C. Fund.*, **3,** 224 (1964).

Tambour, V., and B. Gal-Or, "Phenomenological Theory of Thermodynamic Coupling in Multicomponent Compressible Boundary Layers," *Phys. Fluids.*, **19,** 219 (1976).

Taylor, R., and D. R. Webb, "Film Models for Multicomponent Mass Transfer; Computational Methods: The Exact Solution of the Maxwell-Stefan Equations," *Comp. & Chem. Eng.*, **5,** 61 (1981).

Toor, H. L., "Solutions of the Linearized Equations of Multicomponent Mass Transfer: II. Matrix Methods," *AIChE J.*, **10,** 460 (1964).

Vidwans, A. D., and M. M. Sharma, "Gas-Side Mass Transfer Coefficients in Packed Columns," *Chem. Eng. Sci.*, **22,** 673 (1967).

Vivian, J. E., and C. J. King, "The Mechanism of Liquid-Phase Resistance to Gas Absorption in a Packed Column," *AIChE J.*, **10,** 221 (1964).

Weiss, S., and J. Langer, "Mass Transfer on Valve Trays with Modifications of the Structure of Dispersions," *Distillation, I.Ch.E. Symp. Ser.*, **56,** 2.3/1-26 (1979).

Young, G.C., and J.H. Weber, "Murphree Point Efficiencies in Multicomponent Systems," *I.E.C. Proc. Des. Dev.*, **11,** 440 (1972).

Young, T. C., and W. E. Stewart, "Comparisons of Matrix Approximations for Multicomponent Transfer Calculations," *I.E.C. Fund.*, **25,** 476 (1986).

Zhavoronkov, N.M., V. A. Malynsov, and Y. D. Zel'vensky, "Prediction of Rectification Kinetics Incorporating Heat Exchange between Phases," *Distillation, I.Ch.E. Symp. Ser.*, **56,** 2.1/33-46 (1979).

Manuscript received Nov. 16, 1989, and revision received Feb. 20, 1990.